

## Article

# Metal-Organic Framework Adsorbent Materials in HVAC Systems: General Survey and Theoretical Assessment

Andrea Rocchetti <sup>1,\*</sup>, Martina Lippi <sup>1</sup>, Luca Socci <sup>1</sup>, Paride Gullo <sup>2</sup>, Vahid Khorshidi <sup>3</sup>  
and Lorenzo Talluri <sup>1,\*</sup>

<sup>1</sup> Department of Industrial Engineering, University of Florence, 50139 Florence, Italy

<sup>2</sup> Department of Mechanical and Electrical Engineering, University of Southern Denmark, 6400 Sønderborg, Denmark

<sup>3</sup> RAC R&D Innovation Lab, Danfoss A/S, 6430 Nordborg, Denmark

\* Correspondence: andrea.rocchetti@unifi.it (A.R.); lorenzo.talluri@unifi.it (L.T.)

**Abstract:** In this paper, the use of Metal-Organic Framework (MOF) materials as an option for the energy efficiency enhancement of HVAC systems is investigated. In particular, the possibility of using MOFs as dehumidifying materials to reduce the latent load associated with the moisture content of the airflows is studied. A literature review is proposed, highlighting the benefits of using MOFs instead of other adsorbents (e.g., silica-gel) and discussing the unique features (high water uptake capacity and low regeneration temperatures) that make MOFs a preferential desiccant. The possibility to finely tune these properties is also underlined, reporting some explicative examples. A theoretical proposal of a psychrometric transformation, to be performed in a HVAC system equipped with a MOF-Assisted Dehumidifier (MAD), is presented. This transformation is compared with a traditional one (cooling and dehumidification operated by a cooling coil with low temperatures of the coolant). The preliminary numerical simulations, conducted on a reference case study in Florence, Italy, show an estimated energy saving of 30–50%, leading us to consider the use of this technology as a very competitive one in the air-conditioning sector.

**Keywords:** metal-organic framework; water-uptake; HVAC; dehumidification; energy-saving



**Citation:** Rocchetti, A.; Lippi, M.; Socci, L.; Gullo, P.; Khorshidi, V.; Talluri, L. Metal-Organic Framework Adsorbent Materials in HVAC Systems: General Survey and Theoretical Assessment. *Energies* **2022**, *15*, 8908. <https://doi.org/10.3390/en15238908>

Academic Editors: Alessandro Cannavale and Ubaldo Ayr

Received: 4 November 2022

Accepted: 22 November 2022

Published: 25 November 2022

**Publisher's Note:** MDPI stays neutral with regard to jurisdictional claims in published maps and institutional affiliations.



**Copyright:** © 2022 by the authors. Licensee MDPI, Basel, Switzerland. This article is an open access article distributed under the terms and conditions of the Creative Commons Attribution (CC BY) license (<https://creativecommons.org/licenses/by/4.0/>).

## 1. Introduction

The energy requirements of many countries for refrigeration and air conditioning (AC) systems are dramatically increasing [1–3]. AC devices account for 20–30% of the worldwide electricity consumption of buildings [4,5], which corresponds to at least 10% of global electricity [4]. Considering these numbers and thinking about the non-postponable necessity to reduce electricity consumption and obtain wide-scale decarbonisation, the efficiency enhancement of the AC sector is crucial. AC systems (Heating Ventilation and Air Conditioning, HVAC), ensure thermo-hygrometric comfort in an indoor environment and operate a dehumidification process over the airflow that they treat. The latent heat of the building load (i.e., the water vapour content of the air treated by the system) could account for a great part of the total load (around 30–40%) [6], with greater value in humid climates or in applications where consistent outdoor airflow is required. In traditional HVAC systems, the dehumidification process is driven by a cooling coil (e.g., the evaporator of a Vapour Compression Refrigeration cycle, VCR). To obtain the dehumidification, the coolant of the coil is kept at a temperature much lower than the dew point temperature of the treated airflow, resulting in an over-cooling of the airflow (energy waste) and with a consequent necessity of re-heating. Moreover, these low temperatures of the coolant lead to a low value of the Energy Efficiency Ratio (EER) of the VCR device, with huge electricity consumption. A strategy to minimise the impact of these problems is the utilisation of materials able to remove water vapour contained in the airstream. Between them, an important place is occupied by the adsorbent (or desiccant) materials [7]. Once put in

contact with an airflow, these materials can remove part of the water vapour content from it. In this way, sensible and latent heat could be managed separately [5]. Depending on thermal load and environmental conditions, it is possible to achieve consistent savings. For example, Mazzei et al. showed energy savings of up to 35% using desiccant materials in the HVAC systems of a reference Italian building [8].

Ideally, a sorbent material capable of taking up water from the air should show hydrolytic stability and a relevant adsorption capacity, maintaining its efficient performance over a multitude of uptake-release cycles. Moreover, the regeneration process must require low energy consumption. Desiccant materials act through adsorption processes, taking up water molecules on their surface. This behaviour is well described by the adsorption isotherms, graphs defined by a non-linear relationship between the amount of the adsorbate and the relative humidity measured at defined temperatures. The isotherm trend describes the mass transfer between the aqueous vapour and a porous matter. A suitable material thoughtfully designed for the dehumidification process should be able to adsorb water even at low relative humidity ( $0.05 < RH < 0.40$ ) in order to provide a low energy demanding adsorbent technology. Thereby, a step-function isotherm represents the best adsorption performance.

During the past few decades, the most common adsorbent solids employed for water harvesting have been silica-gels and zeolites [7,9–11]. Concerning the International Union of Pure and Applied Chemistry (IUPAC) classification of physisorption isotherms [12], microporous silica-gels generally present a type II trend, which reflects slow uptake kinetics. On the other hand, although microporous zeolites exhibit a steep uptake tendency at low relative humidity, due to the presence of numerous and strong binding sites for water molecules in their structure, the recovery of the material is energetically costly. Indeed, high temperatures are required to evacuate zeolite porous frameworks from the adsorbed water molecules. This is the main reason for the incomplete degassing process, which translates into low cycling durability for this kind of material [13]. Recently, a zeolite material was proposed as a high-performance water adsorbent, exhibiting fast adsorption kinetic hydrothermal stability, and most importantly, a lower temperature regeneration around  $65\text{ }^{\circ}\text{C}$  [14]. Authors in the paper well characterised the adsorption process, describing how water molecules first coordinate the aluminium centres (at  $RH = 0.01$ ) and then start to fill the 1D pores, forming a dense H-bonding network once the vapour pressure increases; however, defining a mechanism characterized by a low enthalpy value can lead to a low-cost regeneration process. This study explains how the water affinity of the adsorbents drives the adsorption process, maintaining high uptake efficiencies, without increasing the energy consumption for the water desorption. This major challenge can be addressed via a targeted structural design of the material. Consequently, many studies are focusing on the development of tunable materials.

In this regard, very promising adsorbents that are successfully emerging for this purpose have been identified in Metal-Organic Framework (MOF), a class of hybrid organic-inorganic crystalline materials built upon metal-containing units linked to organic ligands through coordination bonds extending within a regular and porous framework. Their robustness, porosity and uncommonly high specific surface area (up to  $6000\text{ m}^2/\text{g}$ ) have made MOFs an attractive proposal in adsorption applications [6,15–17]. Nowadays, theoretical and experimental studies on MOF adsorption abilities have demonstrated great loading and selectivity performances for specific gasses, such as  $\text{CO}_2$  and many volatile organic compounds [18–20]. In this sense, MOFs have gained great consideration for gas-cleaning applications.

MOFs benefit from the possibility of modulating their final properties by a careful design of their reticular structures, thus broadening their range of applications. This representative feature differentiates MOFs from other materials such as their inorganic analogues (i.e., zeolites). The tunability of MOF structures can be exploited to provide suitable adsorption profiles for a high-efficient water capture system (as HVAC airflows dehumidification) [21]. Therefore, owing to their large specific surface area, low frame-

work density and wide-reaching tunable porosity, MOFs can exceed potential traditional microporous adsorbent materials in terms of water adsorption capability. The water adsorption process in a MOF is mediated by chemisorption occurring on the open metal sites, physisorption characterized by the formation of weak interactions with the framework and capillary condensation, which occurs when large pores are present. Since the regeneration of material is strongly connected to these events, tuning the structural properties of the MOF is a valuable pathway to control the desired adsorption and desorption qualities, with the aim of achieving exceptional water harvester systems [22]. Yagi et al. gave efforts to the progress that these functional materials have shown as harvesters for water, mostly in terms of their hydrolytic resilience and their tunable porosity [23]. The Authors underlined the correlation between water uptake and pore volume, emphasizing the need to overcome the energy barrier during the regeneration process of MOF structures displaying large pores. In these cases, hysteresis phenomena are present in water adsorption isotherms, due to irreversible capillarity condensation, responsible for the high-temperature demand for water release. Thus, the pore size should be designed in terms of both high moisture capture capacity and relatively easy material regeneration, for example, by modulating the length of the organic linker or by introducing chemical functionalization during post-synthetic modification [24].

It is crucial to understand the water uptake mechanism by evaluating how the water molecules populate their binding sites within the MOF structure. In this sense, X-ray diffraction in combination with Density-Functional Theory calculations can be appropriate tools, as demonstrated by Hanikel et al. with the studies performed on MOF-303, which exhibits water adsorption with a steep trend at very low RH [25]. Understanding the hierarchically filling of the pores was demonstrated to be essential in order to induce a more adequate water uptake behaviour. In particular, they proposed a multivariate approach for the modification of the architecture of the pores, finding the most appropriate material design in compliance with the water adsorption enthalpy values, the limiting desorption temperature, the stability and the water capacity. In addition, the condition of the adsorption mechanism can be varied to understand the mechanism of water harvesting as was reported by Yanagita et al. [26]. In detail, they measured the adsorption/desorption isotherms of chromium terephthalate MIL-101 and the time trend of the amount of adsorbed water by stepwise modification of the relative humidity, describing how the porosity and the hydrophobic-hydrophilic structural composition of the MOFs drive the uptake/release kinetic of the water. Based on these all considerations, it is evident that a proper design of the material is a reasonable strategy to allow a successful material development for water uptake applications.

In the literature, it is possible to find few works that deal with the utilisation of MOF materials as desiccants in HVAC applications. Some of them propose using the traditional desiccant wheels coated with MOF materials. Bareschino et al. performed a numerical simulation of a desiccant wheel with MOF MIL-101 [27], including a gas-side resistance model to define the behaviour of MOF material. Dehumidification effectiveness of 30% better than the silica-gel wheel is demonstrated. The Authors estimated a reduction of 20.5% in CO<sub>2</sub> emissions compared to the HVAC system with silica-gel. Shahvari et al. explained the functioning of a MOF desiccant wheel [15], proposing a complete first-principle analysis validated with experimental tests. They showed that MOF-based wheels are regenerable at lower temperatures (40–60 °C) compared to silica-gel (80–140 °C), with consistent energy saving for regeneration (10–50%, depending on environmental conditions). Shahvari obtained promising results for a system that integrates MOF-assisted dehumidification with indirect evaporative cooling [28]. Again, the low regeneration temperatures (40–75 °C) have been confirmed, with consequent gain in the efficiency of the MOF system with respect to the silica-gel system (MOF system has an efficiency 2.7–6 times higher). The idea of using MOF-coated desiccant wheels has been well-reviewed and studied, as in the publication [29] and in the work of Wang [30], where the MOF materials are cited as

good desiccant options due to their low regeneration temperatures (30–60 °C). Cui et al. proposed to coat the surface of the coils of a VCR cycle with MIL-100 (Fe) (Figure 1), [6].

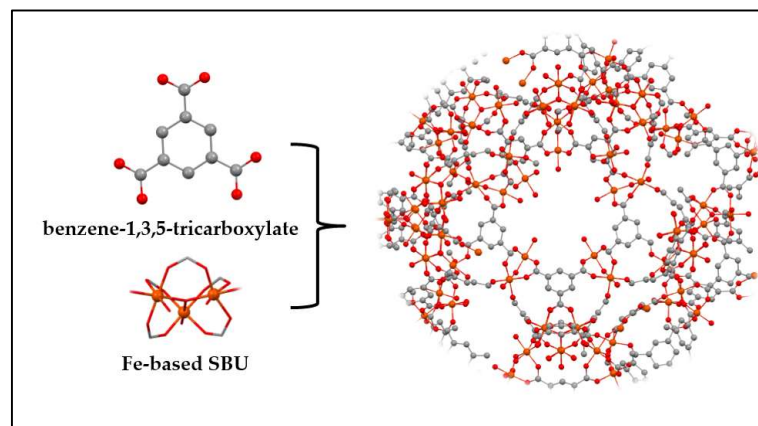


**Figure 1.** Crystal structure of MIL100(Fe) from the reaction between the benzene-1,3,5-tricarboxylate and the iron(III)-based cluster.

In adsorption mode, the evaporator acts as a cooler and dehumidifier while the waste heat of the condenser regenerates the wet MOF. The MOF-coated evaporator removes at the same time as the sensible and latent heat of the airflow, operating an isothermal-dehumidification. In the paper, the low regeneration temperature of the material (about 50 °C) is highlighted. With a theoretical EER of 7.9 in typical European summer conditions, the estimated energy-saving is 36.0% compared to traditional dehumidification with a cooling coil. The idea of coating a heat exchanger with desiccant material has been reported by review papers of Saeed et al. [31] and Venegas et al. [32], which considered MOFs as material to be used for the purpose. Even if this solution is not directly applied in the HVAC system, it is important to cite in the context of the control of thermo-hygrometric parameters of indoor environments and the energy-enhancement of HVACs, which was proposed by Feng et al. [16]. They proposed, in accordance with the results of a lumped-model simulation, to install a MIL-100 (Fe) in an indoor environment with the role of a moisture buffer; the removal of indoor humidity accounts for 73.4% of latent heat, leading to minor efforts of the HVAC system.

In this paper, the Authors theoretically compare a HVAC system that operates traditional dehumidification with a HVAC system equipped with a MOF-Assisted Dehumidifier (MAD). First of all, the reference psychrometric transformations are shown. Then, the mathematical model used in the simulations is presented. The two kinds of dehumidification are compared by considering a case study, based on real boundary conditions. The benefits, in terms of energy consumption, that characterise MOF-assisted dehumidification are quantified, also highlighting better results obtainable with MOF materials compared to other desiccant materials, in terms of consumption for the regeneration process. The obtained results lead the Authors to consider this technology as a very competitive option in the HVAC sector, and it inspires us to further research this topic.

## 2. Traditional Dehumidification vs. MOF-Assisted Dehumidification: Psychrometric Transformations

The proposed MOF-assisted dehumidification is compared here, in terms of reference psychrometric transformations, with a traditional dehumidification process operated by a cooling coil. In both cases, the setpoint indoor conditions are reached from the supply conditions, ensured by the HVAC system, considering the sensible and latent thermal loads.

### 2.1. HVAC with Traditional Dehumidification

In a HVAC system with traditional dehumidification (Figure 2), the dehumidification process is operated by a cooling coil.

- Pre-cooling of the outdoor air with an air-to-air heat exchanger, where the exhaust airflow coming from indoors is used as a pre-cooling medium (transformation 1–2).
- Cooling and dehumidification with a cooling coil (with a low temperature of the coolant). The air at the outlet of the coil is saturated, and the temperature is equal to the dew point temperature of the supply conditions (2–3). Coolant temperature must be lower than this limit. Additionally, in HVAC applications, a reference temperature for the coolant entering the coil is 7 °C.
- Heating with a post-heating coil (e.g., the desuperheater and/or condenser of the VCR, or other thermal sources) to reach supply conditions (3–4).

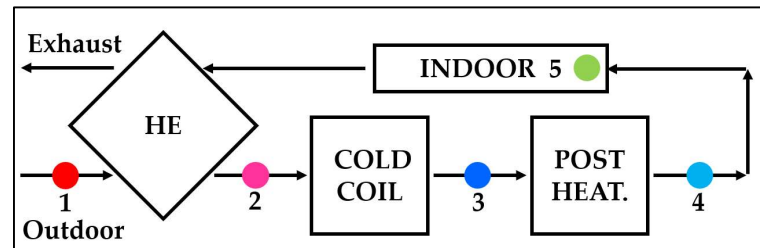


Figure 2. Schematic representation of a HVAC system with traditional dehumidification.

A generic complete process is represented in Figure 3.

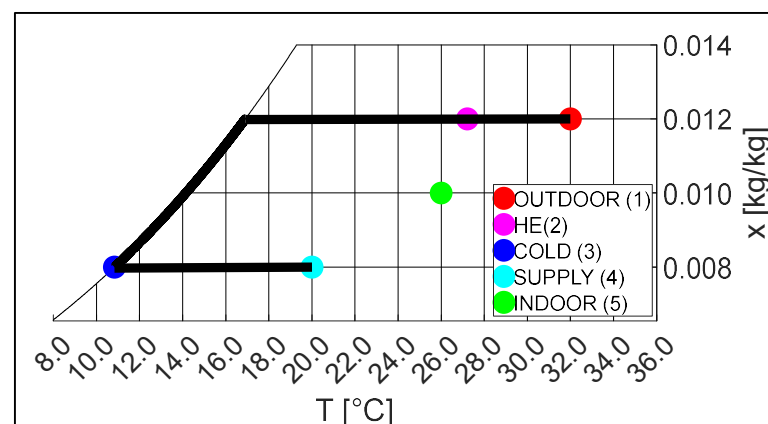


Figure 3. Transformations in an HVAC system with traditional dehumidification.

## 2.2. HVAC with MOF-Assisted Dehumidification

In a HVAC system with MOF-assisted dehumidification (Figure 4), the dehumidification process is operated by a device that connects the outdoor airflow with the MOF material, ensuring an isothermal transformation. In the system, the outdoor airflow undergoes the following transformations:

- Isothermal dehumidification with a MOF-Assisted Dehumidifier (MAD). The final point of the dehumidification process has a humidity ratio equal to the ones of supply conditions (transformations).
- Sensible cooling with the cooling coil, with a higher temperature of the coolant. In this case the coolant temperature must be lower than the air at the coil outlet, but these values are significantly higher than in the traditional cooling/dehumidification process.

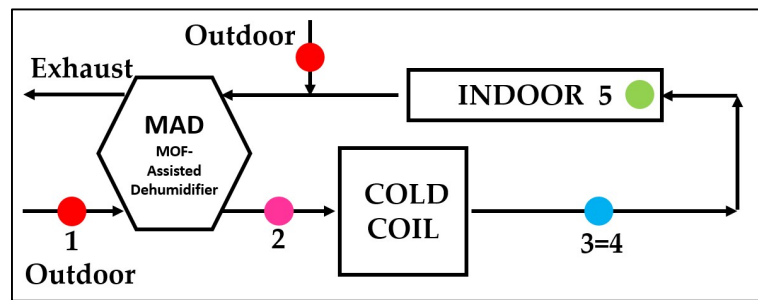


Figure 4. Schematic representation of a HVAC system with MOF-assisted dehumidification.

A generic complete process is represented in Figure 5.

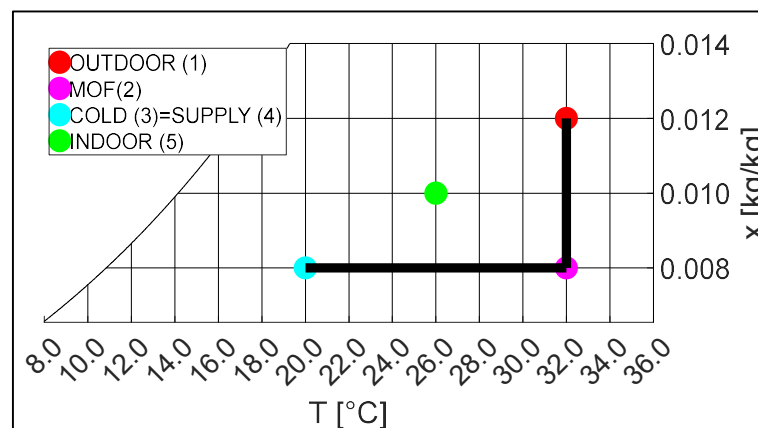


Figure 5. Transformations in a HVAC system with MOF-assisted dehumidification.

This description refers to the adsorption process. This process generates heat, which must be removed to obtain isothermal dehumidification of the airflow. Otherwise, the airflow will undergo an isenthalpic transformation, with a hypothetical consistent rise of its temperature (typical psychrometric transformation of desiccant wheels). Therefore, a cooling medium is necessary to avoid the heating of the system. For this purpose, it should use an airflow resulting from a mix between the exhausted airflow extracted from the indoor environment and an additional outdoor airflow. This mix will have a temperature within the same range as points one and five (Figures 3 and 5).

For the regeneration (that is not described in this paper), it is supposed that the utilisation of an outdoor airflow will be heated by the condenser of the VCR (e.g., at temperature  $T_{II}$ , Figure 6).

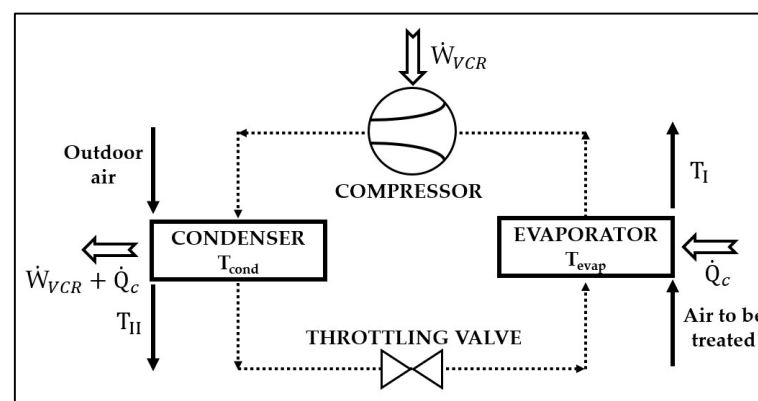


Figure 6. Reference scheme for the VCR cycle.

### 3. Mathematical Modelling

In the following, a simplified mathematical model used for the evaluation of the different psychrometric transformations is shown. The supply airflow is formed completely by outdoor air. The supply conditions, in terms of temperature and humidity ratio, are defined as follows:

$$T_s = T_i - \frac{\dot{Q}_{sens}}{c * \dot{m}} \quad (1)$$

$$x_s = x_i - \frac{\dot{Q}_{lat}}{r * \dot{m}} \quad (2)$$

where the constant pressure specific heat of air  $c$  is assumed equal to 1.0 kJ/(kg\*K) and the latent heat of vaporisation of water  $r$  is assumed equal to 2500.0 kJ/kg.

In the different scenarios object of the analysis, the repartition between sensible and latent heat has been changed according to the Sensible Heat Ratio (SHR) parameter:

$$SHR = \frac{\dot{Q}_{sens}}{\dot{Q}_{sens} + \dot{Q}_{lat}} \quad (3)$$

#### 3.1. HVAC with Traditional Dehumidification

The air-to-air heat exchanger is modelled with the Kays and London efficiency:

$$eff_{HE} = \frac{T_o - T_{he}}{T_o - T_e} \quad (4)$$

where the outdoor airflow, that must be treated, is cooled by the same quantity of exhaust airflow (characterised by the same thermo-hygrometric conditions as the indoor environment).

The condition at the outlet of the cooling coil corresponds to a saturation condition, corresponding to the dew point state of the supply air:

$$T_c = T_{dp,s} \quad (5)$$

$$x_c = x_s \quad (6)$$

The cooling power provided by the cooling coil (e.g., the cooling power provided by the evaporator of VCR in this context) is equal to:

$$\dot{Q}_c = \dot{m} * (j_{he} - j_c) \quad (7)$$

To evaluate the electric power consumption of the VCR cycle, associated with the activation of the cooling coil, the temperature levels of the coolant must be considered. They are set by the air temperature conditions at the cooling coil (evaporator) and at the condenser, and by opportune temperature differences between coolant and air (Figure 6). For the evaporator, the outlet air temperature is known ( $T_I$ , equal to  $T_c$  in this context), consequently the evaporation temperature; for the condenser, an outlet condensing air temperature is fixed ( $T_{II}$ ), consequently the condensation temperature. The temperature differences at the evaporator and the condenser ( $DT_{evap}$  and  $DT_{cond}$ ) are defined, taking into account common efficiencies for these kinds of heat exchangers:

$$T_{evap} = T_I - DT_{evap} \quad (8)$$

$$T_{cond} = T_{II} + DT_{cond} \quad (9)$$

Once the refrigerant levels are defined, it is possible to evaluate the EER of the VCR with parametric functions of  $T_{evap}$  and  $T_{cond}$ , obtained by analyzing some commercial models [33]. Then, the power consumption of the VCR cycle is:

$$\dot{W}_{VCR} = \frac{\dot{Q}_c}{EER} \quad (10)$$

The necessary heating power, to bring the air to the supply conditions, is:

$$\dot{Q}_h = \dot{m} * (j_h - j_c) \quad (11)$$

### 3.2. HVAC with MOF-Assisted Dehumidification

At the MOF device, the outdoor air undergoes isothermal dehumidification down to the supply humidity ratio.

The condition at the outlet of the cooling coil corresponds to the supply conditions.

The cooling power provided by the cooling coil (e.g., evaporator of VCR) is:

$$\dot{Q}_c = \dot{m} * (j_{mof} - j_s) \quad (12)$$

The power consumption of the VCR cycle is calculated as previously explained. It is possible to observe from Figure 5 that, in this case, the temperature of refrigerant can be kept higher, resulting in favourable conditions for the VCR performance.

In this case, no heating power is required to bring the airflow to supply conditions.

## 4. Case Study

The selected case study is based on a reference building located in Florence, Italy, served by a HVAC system. Locale climate conditions for typical summer days have been considered (Table 1, derived from ASHRAE [34] and Italian Standards [35] indications). The indoor setpoint conditions, the number of people present in the building (which is relevant to define the repartition between sensible and latent thermal load) and the necessary outdoor air have been chosen according to the Italian technical standards for thermo-hygrometric comfort and building management (Table 2) [35].

**Table 1.** Outdoor air conditions assumed in the simulations.

CASE	$T_o$ [°C]	$RH_o$ [%]
A	35.0	30.0
B	33.5	45.0

**Table 2.** Boundary conditions assumed in the simulations (part 1).

$T_i$ [°C]	26.0
$RH_i$ [%]	50.0
n	80
$\dot{m}_p$ [kg/s/s]	0.0125
$\dot{m}$ [kg/s]	1.0
$\dot{Q}_{sens,p}$ [W]	50.0
$\dot{Q}_{lat,p}$ [W]	50.0

Three different scenarios of thermal load, with different supply air conditions (Equations (1) and (2)), have been considered (Table 3). In the following table, the latent load is related to the presence of people, and the sensible one has been varied according to some SHRs. Thus, the sensible and latent loads do not refer to the loads that derive from ventilation.



**Table 3.** Boundary conditions used in the simulations (part 2).

SCENARIO	SHR	$\dot{Q}_{\text{sens}}$ [kW]	$\dot{Q}_{\text{lat}}$ [kW]	$T_s$ [°C]	$x_s$ [kg/kg]
1	0.50	4.0	4.0	22.0	0.009
2	0.60	6.0	4.0	20.0	0.009
3	0.67	8.0	4.0	18.0	0.009

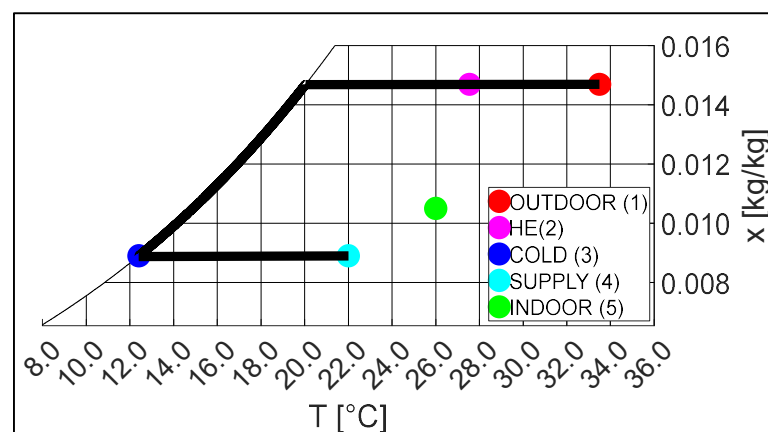
## 5. Results and Discussion

In the following, MOF-assisted dehumidification is compared with the dehumidification operated by a traditional HVAC system. Then, some comparisons between the performances of MOFs as desiccants and traditional desiccant materials (i.e., silica-gel) are proposed.

### 5.1. Comparison of Psychrometric Transformations

The following figures show the psychrometric transformations (for outdoor conditions of case B) that the airflow undergoes in the HVAC with traditional dehumidification and in the HVAC with MOF-assisted dehumidification.

From these figures, apart from the energy savings that will be discussed in the following parts, a crucial point emerges. The lowest temperatures of the airflow are set as follows: the supply dew point temperature in the traditional dehumidification is about 12.0 °C, Figure 7, and the supply temperature in the MOF-assisted dehumidification is 22.0 °C, Figure 8. This fact has important consequences: there is a temperature difference of 10.0 °C in the evaporation temperature of the VCR in the two systems (assuming the same temperature difference evaporating coolant-outlet air), with a general gain in EER for the second configuration. In any case, in the following calculations, the gain in EER is partially penalized by the necessity to have slightly hotter air exiting the condenser ( $T_{II}$ , Figure 6) to enhance the regeneration process. This assumption has been made to obtain more reliable results, taking into consideration possible parasitic phenomena in the regeneration process, even if, according to the literature [6], no higher condensing coolant temperature, with respect to the traditional HVAC, is needed.

**Figure 7.** Transformations for HVAC with traditional dehumidification (case B, scenario 1).

### 5.2. Comparison between Traditional and MOF-Assisted Dehumidification

It is possible to compare the different configurations in terms of cooling power provided by the cooling coil, consequently in terms of electrical power consumption of the VCR (Table 4). The cooling power required in the different scenarios is always the same for the HVAC with traditional dehumidification, because the cooling coil must cool down the inlet air to the dew point temperature of the supply air. In the last column, the savings compared to the traditional configuration are reported.

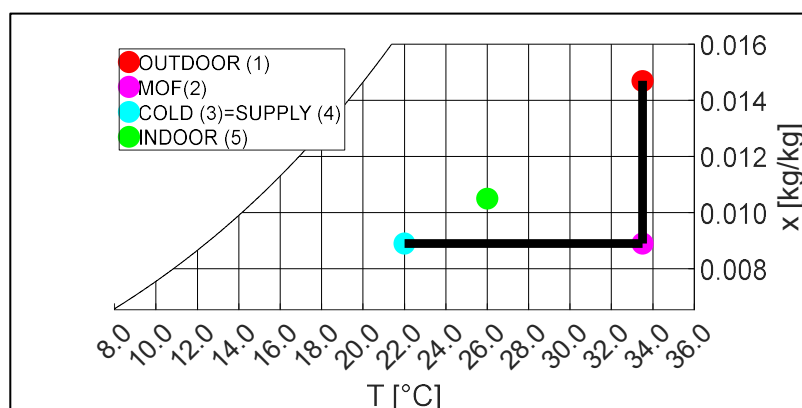


Figure 8. Transformations for HVAC with MOF-assisted dehumidification (case B, scenario 1).

Table 4. Cooling power and electric power consumption for the two HVAC configurations.

CASE	SCENARIO	$\dot{Q}_c$ [kW] TRAD.	$\dot{W}_{VCR}$ [kW] TRAD.	$\dot{Q}_c$ [kW] MOF	$\dot{W}_{VCR}$ [kW] MOF	Savings [%]
A	1	19.9	6.2	13.2	3.6	41.9
	2	19.9	6.2	15.2	4.3	30.6
	3	19.9	6.2	17.2	5.2	16.1
B	1	30.2	9.6	11.7	3.3	65.6
	2	30.2	9.6	13.7	4.2	56.3
	3	30.2	9.6	15.7	5.1	46.9

Comparing the respective scenarios for both cases, and mediating the values, it is possible to assert that the energy savings with MOF dehumidification is in the range of 30–50%.

### 5.3. Comparison between MOF and Other Desiccants

As already explained in the introduction, isotherm profiles analysis can be a good approach to show the benefits of MOFs with respect to other common desiccants, in terms of adsorbate/adsorbent mass ratio and temperature required for regeneration. In the following figures, the isotherms of good examples belonging to the three main classes of desiccants are reported:

- A common silica-gel [36].
- A recently reported zeolite [14].
- One of the best performant MOFs, e.g., MIL-100 (Fe) [6].

In the graphs, the water uptake (adsorbed water mass/adsorbent mass) is reported as a function of vapour pressure (instead of relative humidity, as described in the introduction), in order to clearly show the adsorption behaviour at different temperatures.

In each graph (Figures 9–11), the isotherms corresponding to the adsorption ( $T_o = 33.5$  °C of case B) and typical regeneration temperatures are reported. For silica-gel and zeolite the isotherm associated with the temperature of the air exiting the condenser of VCR ( $T_{II}$ ) is shown, to make an easy comparison with MOF material.

Considering the boundary conditions of case B ( $T_o = 33.5$  °C,  $RH_o = 45.0\%$ ) and the regeneration temperature indicated in [6,14,36], the obtained results are resumed in Table 5:

Table 5. Uptake and regeneration characteristics of the material under comparison.

MATERIAL	$u$ [kg/kg]	$T_{reg}$ [°C]
Silica-gel	0.24	90.0
Zeolite	0.30	65.0
MOF MIL-100	0.48	50.0

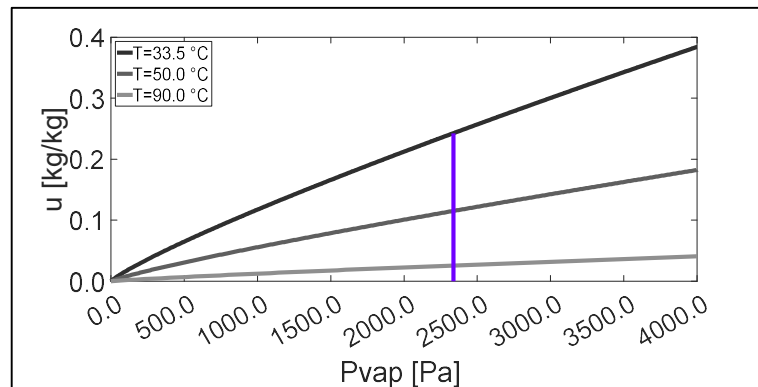


Figure 9. Isotherms of silica-gel under analysis [36].

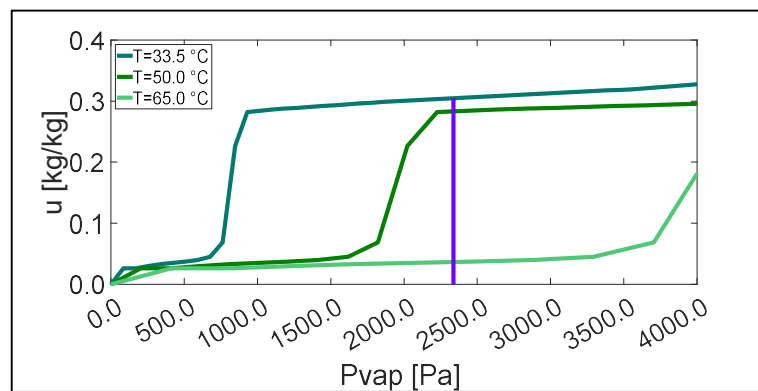


Figure 10. Isotherms of zeolite [14].

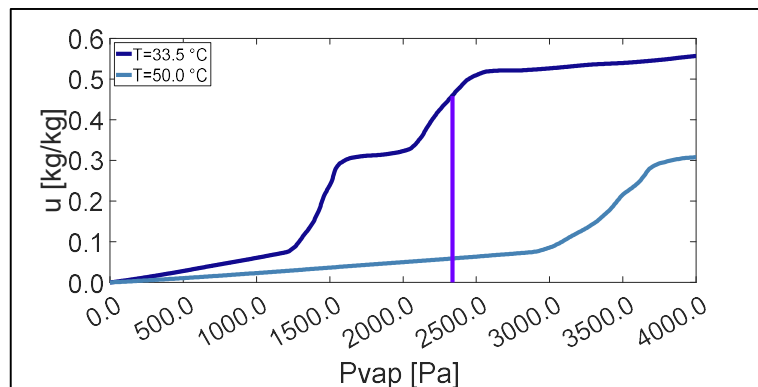


Figure 11. Isotherms of MOF MIL-100 (Fe) [6].

It is possible to note that MOF material shows the best performance of water uptake at these conditions (0.48 kg/kg against 0.24 kg/kg of silica-gel and 0.30 kg/kg of zeolite). This means that, for the same used quantity of adsorbent material and the same boundary conditions, MOF material achieves a better dehumidification result (i.e., amount of water vapour adsorbed). These results are representative of a typical situation in which air dehumidification is required. Generally speaking, MOF materials have a favourable isotherm, so they are strongly effective, in the range of sufficiently high values of RH that otherwise would request an overload on the cooling device (e.g., low coolant temperatures) for the dehumidification process. Regarding the regeneration capacity, it is useful to compare in the graphs the temperatures required to obtain a value of uptake close to zero. MIL-100 presents, compared to the other options, a low regeneration temperature to remove the uptake water content from the material and restore its adsorption capacity. It is vital to

remark that this temperature is well coupled with the conditions of the VCR condenser (low-grade thermal energy), while additional heat sources are requested for the other desiccants (as it is possible to observe from Figures 9–11).

## 6. Conclusions

In this paper, the importance of using desiccant materials for the energy enhancement of HVAC systems has been discussed. Desiccant materials can dehumidify the airflows, removing the latent heat, with better performances of cooling devices and consequent energy savings. Among the many available materials, attention has been addressed to Metal-Organic Framework (MOF) materials, which have unique adsorption characteristics (high water uptake, low regeneration temperatures) compared to other known desiccants (i.e., silica-gel).

In the first part of the paper, a general overview of MOFs is presented, in particular emphasising the possibility to control the design of their structures, aimed at the desired properties. Moreover, the application of MOFs in the HVAC context has been reviewed. The literature analysis shows that the big advantage of MOFs over silica-gel is the low regeneration temperature (40–60 °C against 90–100 °C). The proposed solutions are the desiccant wheel and exchangers coated with MOFs and cooled by a refrigerant.

Then, a comparison between a traditional HVAC (with dehumidification operated by a cooling coil) and a HVAC equipped with a MOF-Assisted Dehumidifier (MAD) has been discussed. The mathematical model of the two HVAC alternatives is applied to a real case study. The energy savings achievable with MOF dehumidification are in the range of 30–50%, depending on the outdoor air conditions and the repartition between sensible and latent heat. Comparing the MOF material with other desiccants (silica-gel and a new zeolite), the MOF-driven dehumidification shows the highest water uptake and the lowest regeneration temperature. The obtained results lead us to consider the utilisation of MOF-assisted dehumidification as a very competitive strategy to reduce the energy consumption of the HVAC sector, making decarbonization closer, and inspiring the Authors to make deeper studies on this topic.

**Author Contributions:** Conceptualization, A.R., L.S. and L.T.; Methodology, M.L. and L.S.; Software, L.S.; Validation, L.S.; Formal analysis, M.L. and L.S.; Investigation, M.L. and L.S.; Resources, A.R.; Data curation, M.L. and L.S.; Writing—original draft, L.S.; Writing—review & editing, A.R., M.L., L.S. and L.T.; Supervision, A.R., P.G., V.K. and L.T.; Project administration, P.G. and L.T.; Funding acquisition, A.R., P.G., V.K. and L.T. All authors have read and agreed to the published version of the manuscript.

**Funding:** This research received no external funding.

**Conflicts of Interest:** The authors declare no conflict of interest.

## Abbreviations

AC	Air Conditioning
$c$	Constant pressure specific heat [kJ/kg/K]
DT	Temperature difference [°C]
EER	Energy Efficiency Ratio
eff	Efficiency
HVAC	Heating Ventilation Air Conditioning
$j$	Specific enthalpy [kJ/kg]
$\dot{m}$	Air mass flow rate [kg/s]
MAD	MOF-Assisted Dehumidifier
MOF	Metal-Organic Framework
$n$	Number of people

$\dot{Q}$	Thermal load [kW]
$r$	Latent heat of vaporisation [kJ/kg]
RH	Relative Humidity [%]
SHR	Sensible Heat Ratio
$T$	Temperature [°C]
$u$	Water uptake [kg water/kg adsorbent]
VCR	Vapour Compression Refrigeration
$\dot{W}$	Power [kW]
$x$	Humidity ratio [kg/kg]
Subscripts	
$c$	Cooling coil
$dp$	Dew point
$e$	Exhaust airflow (from indoor environment)
$h$	Heating coil
$he$	Air-to-air heat exchanger
$i$	Indoor air
$lat$	Latent
$mof$	MOF-Assisted Dehumidifier
$o$	Outdoor air
$p$	Person
$s$	Supply air
$sens$	Sensible
$evap$	Evaporator of the VCR cycle
$cond$	Condenser of the VCR cycle
$I$	Air at the outlet of the evaporator
$II$	Air at the outlet of the condenser

## References

- Grazzini, G.; Milazzo, A. *Tecnica Del Freddo*; Società Editrice Esculapio: Bologna, Italy, 2017; ISBN 9788874889969.
- IEA. World Energy Outlook 2022. IEA Report. 2022. Available online: <https://www.iea.org/reports/world-energy-outlook-2022> (accessed on 21 November 2022).
- IEA. Net Zero by 2050. IEA Report. 2021. Available online: <https://www.iea.org/reports/net-zero-by-2050> (accessed on 21 November 2022).
- IEA. The future of cooling. IEA Report. 2018. Available online: <https://www.iea.org/reports/the-future-of-cooling> (accessed on 21 November 2022).
- Zaki, O.M.; Mohammed, R.H.; Abdelaziz, O. Separate sensible and latent cooling technologies: A comprehensive review. *Energy Convers. Manag.* **2022**, *256*, 115380. [[CrossRef](#)]
- Cui, S.; Qin, M.; Marandi, A.; Steggles, V.; Wang, S.; Feng, X.; Nouar, F.; Serre, C. Metal-Organic Frameworks as advanced moisture sorbents for energy-efficient high temperature cooling. *Sci. Rep.* **2018**, *8*, 15284. [[CrossRef](#)] [[PubMed](#)]
- Sultan, M.; El-Sharkawy, I.I.; Miyazaki, T.; Saha, B.B.; Koyama, S. An overview of solid desiccant dehumidification and air conditioning systems. *Renew. Sustain. Energy Rev.* **2015**, *46*, 16–29. [[CrossRef](#)]
- Mazzei, P.; Minichiello, F.; Palma, D. Desiccant HVAC systems for commercial buildings. *Appl. Therm. Eng.* **2002**, *22*, 545–560. [[CrossRef](#)]
- Ng, E.P.; Mintova, S. Nanoporous materials with enhanced hydrophilicity and high water sorption capacity. *Microporous Mesoporous Mater.* **2008**, *114*, 1–26. [[CrossRef](#)]
- LaPotin, A.; Zhong, Y.; Zhang, L.; Zhao, L.; Leroy, A.; Kim, H.; Rao, S.R.; Wang, E.N. Dual-Stage Atmospheric Water Harvesting Device for Scalable Solar-Driven Water Production. *Joule* **2021**, *5*, 166–182. [[CrossRef](#)]
- Goldsworthy, M.J. Measurements of water vapour sorption isotherms for RD silica gel, AQSOA-Z01, AQSOA-Z02, AQSOA-Z05 and CECA zeolite 3A. *Microporous Mesoporous Mater.* **2014**, *196*, 59–67. [[CrossRef](#)]
- Thommes, M.; Kaneko, K.; Neimark, A.V.; Olivier, J.P.; Rodriguez-Reinoso, F.; Rouquerol, J.; Sing, K.S.W. Physisorption of gases, with special reference to the evaluation of surface area and pore size distribution (IUPAC Technical Report). *Pure Appl. Chem.* **2015**, *87*, 1051–1069. [[CrossRef](#)]
- Castillo, J.M.; Silvestre-Albero, J.; Rodriguez-Reinoso, F.; Vlugt, T.J.H.; Calero, S. Water adsorption in hydrophilic zeolites: Experiment and simulation. *Phys. Chem. Chem. Phys.* **2013**, *15*, 17374–17382. [[CrossRef](#)]
- Liu, Z.; Xu, J.; Xu, M.; Huang, C.; Wang, R.; Li, T.; Huai, X. Ultralow-temperature-driven water-based sorption refrigeration enabled by low-cost zeolite-like porous aluminophosphate. *Nat. Commun.* **2022**, *13*, 193. [[CrossRef](#)]
- Shahvari, S.Z.; Kalkhorani, V.A.; Wade, C.R.; Clark, J.D. Benefits of metal-organic frameworks sorbents for sorbent wheels used in air conditioning systems. *Appl. Therm. Eng.* **2022**, *210*, 118407. [[CrossRef](#)]

16. Feng, X.; Qin, M.; Cui, S.; Rode, C. Metal-organic framework MIL-100(Fe) as a novel moisture buffer material for energy-efficient indoor humidity control. *Build. Environ.* **2018**, *145*, 234–242. [[CrossRef](#)]
17. Ming, Y.; Kumar, N.; Siegel, D.J. Water Adsorption and Insertion in MOF-5. *ACS Omega* **2017**, *2*, 4921–4928. [[CrossRef](#)] [[PubMed](#)]
18. Hu, Z.; Wang, Y.; Shah, B.B.; Zhao, D. CO<sub>2</sub> Capture in Metal-Organic Framework Adsorbents: An Engineering Perspective. *Adv. Sustain. Syst.* **2019**, *3*, 1800080. [[CrossRef](#)]
19. González-Zamora, E.; Ibarra, I.A. CO<sub>2</sub> capture under humid conditions in metal-organic frameworks. *Mater. Chem. Front.* **2017**, *1*, 1471–1484. [[CrossRef](#)]
20. Li, H.-Y.; Zhao, S.-N.; Zang, S.-Q.; Li, J. Functional metal-organic frameworks as effective sensors of gases and volatile compounds. *Chem. Soc. Rev.* **2020**, *49*, 6364–6401. [[CrossRef](#)]
21. LaPotin, A.; Kim, H.; Rao, S.R.; Wang, E.N. Adsorption-Based Atmospheric Water Harvesting: Impact of Material and Component Properties on System-Level Performance. *Acc. Chem. Res.* **2019**, *52*, 1588–1597. [[CrossRef](#)]
22. Zhou, X.; Lu, H.; Zhao, F.; Yu, G. Atmospheric Water Harvesting: A Review of Material and Structural Designs. *ACS Mater. Lett.* **2020**, *2*, 671–684. [[CrossRef](#)]
23. Hanikel, N.; Prévot, M.S.; Yaghi, O.M. MOF water harvesters. *Nat. Nanotechnol.* **2020**, *15*, 348–355. [[CrossRef](#)]
24. Khutia, A.; Rammelberg, H.U.; Schmidt, T.; Henninger, S.; Janiak, C. Water sorption cycle measurements on functionalized MIL-101Cr for heat transformation application. *Chem. Mater.* **2013**, *25*, 790–798. [[CrossRef](#)]
25. Hanikel, N.; Pei, X.; Chhedha, S.; Lyu, H.; Jeong, W.; Sauer, J.; Gagliardi, L.; Yaghi, O.M. Evolution of water structures in metal-organic frameworks for improved atmospheric water harvesting. *Science* **2021**, *374*, 454–459. [[CrossRef](#)]
26. Yanagita, K.; Hwang, J.; Shamim, J.A.; Hsu, W.-L.; Matsuda, R.; Endo, A.; Delaunay, J.-J.; Daiguji, H. Kinetics of Water Vapor Adsorption and Desorption in MIL-101 Metal-Organic Frameworks. *J. Phys. Chem. C* **2019**, *123*, 387–398. [[CrossRef](#)]
27. Bareschino, P.; Diglio, G.; Pepe, F.; Angrisani, G.; Roselli, C.; Sasso, M. Numerical study of a MIL101 metal organic framework based desiccant cooling system for air conditioning applications. *Appl. Therm. Eng.* **2017**, *124*, 641–651. [[CrossRef](#)]
28. Shahvari, S.Z.; Kalkhorani, V.A.; Clark, J.D. Performance evaluation of a metal organic frameworks based combined dehumidification and indirect evaporative cooling system in different climates. *Int. J. Refrig.* **2022**, *140*, 186–197. [[CrossRef](#)]
29. Affordable and Sustainable Cooling Using Metal-Organic Frameworks. Catalyzing Commercialization. Available online: <https://www.aiche.org/sites/default/files/cep/20200916.pdf> (accessed on 21 November 2022).
30. Wang, W.; Wu, L.; Li, Z.; Fang, Y.; Ding, J.; Xiao, J. An Overview of Adsorbents in the Rotary Desiccant Dehumidifier for Air Dehumidification. *Drying Technol.* **2013**, *31*, 1334–1345. [[CrossRef](#)]
31. Saeed, A.; Al-Alili, A. A review on desiccant coated heat exchangers. *Sci. Technol. Built Environ.* **2017**, *23*, 136–150. [[CrossRef](#)]
32. Venegas, T.; Qu, M.; Nawaz, K.; Wang, L. Critical review and future prospects for desiccant coated heat exchangers: Materials, design, and manufacturing. *Renew. Sustain. Energy Rev.* **2021**, *151*, 111531. [[CrossRef](#)]
33. Danfoss. CoolSelector Software. Available online: <https://www.danfoss.com/en-gb/service-and-support/downloads/dcs/coolselector-2/> (accessed on 21 November 2022).
34. ASHRAE. *ASHRAE Handbook-Fundamentals*; ASHRAE: Atlanta, GA, USA, 2021.
35. *Standard UNI 10339:1995*; Air-conditioning systems for thermal comfort in buildings. General, classification and requirements. Offer, order and supply specifications. UNI Ente Nazionale di Normazione: Milano, Italy, 1995.
36. Mohammed, R.H.; Mesalhy, O.; Elsayed, M.L.; Su, M.; Chow, L.C. Revisiting the adsorption equilibrium equations of silica-gel/water for adsorption cooling applications. *Int. J. Refrig.* **2018**, *86*, 40–47. [[CrossRef](#)]